

DISCOVERY OF TRIKETONE-QUINOXALINE HYBRIDS AS POTENT HPPD INHIBITORS USING STRUCTURE-BASED DRUG DESIGN

Baifeng ZHENG*, Yaochao YAN*, Can FU, Guangyi HUANG, Long ZHAO, Qiong CHEN (✉), Renyu QU (✉), Guangfu YANG

Key Laboratory of Pesticides & Chemical Biology of the Ministry of Education, International Joint Research Center for Intelligent Biosensor Technology and Health, College of Chemistry, Central China Normal University, Wuhan 430079, China.

*These authors contribute equally to the work

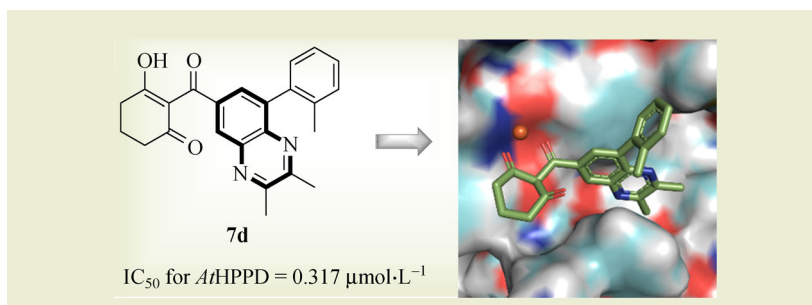
KEYWORDS

herbicide, HPPD, inhibitor, quinoxaline, triketone

HIGHLIGHTS

- HPPD is one of the most promising targets for new herbicides.
- A family of novel HPPD inhibitors based on the triketone-quinoxaline scaffold was designed and synthesized.
- One particular product (7d) gave the highest inhibition of HPPD of the newly synthesized derivatives.
- Triketone-quinoxaline derivatives provide a useful molecular scaffold for the discovery of novel HPPD-inhibiting herbicides.

GRAPHICAL ABSTRACT



ABSTRACT

p-Hydroxyphenylpyruvate dioxygenase (EC 1.13.11.27, HPPD) belongs to the family of Fe(II)-dependent non-heme oxygenases that occur in the majority of aerobic organisms. HPPD has proved to be a promising target in herbicide research and development. A battery of novel triketone-quinoxaline compounds has been designed using a structure-based drug design strategy and then prepared. Enzyme inhibition assays show that these synthesized derivatives possess favorable inhibition capability against *Arabidopsis thaliana* HPPD with IC₅₀ values ranging from 0.317 to 0.891 μmol·L⁻¹. Subsequently, the molecular docking results indicate that two adjacent carbonyls of the triketone moiety of the representative compound 2-(2,3-dimethyl-8-(*o*-tolyl)quinoxaline-6-carbonyl)-3-hydroxycyclohex-2-en-1-one (7d) engage in chelation with the ferrous ion of *A. thaliana* HPPD in a bidentate pose, and its quinoxaline scaffold forms two sets of parallel π-stacking interaction between two phenylalanine residues (Phe424 and Phe381). In addition, the extended phenyl group also interacts with Phe392 in a π-π stacking way. This study indicates that triketone-quinoxaline is a promising scaffold for discovering HPPD inhibitors with substantially increased potency, providing insight into the molecular design of new herbicides.

Received January 31, 2021;

Accepted March 31, 2021.

Correspondences: qchen@mail.ccnu.edu.cn,
renyu@mail.ccnu.edu.cn

1 INTRODUCTION

Herbicides have made an irreplaceable contribution in ensuring crop production and safety over recent decades^[1]. However, due to irrational and excessive use of herbicides the development of resistance in target weeds to herbicides has become increasingly rapid and widespread^[2]. There is therefore an urgent need to develop novel herbicides with new modes of action, and this is the most efficient path to overcoming the current problem of weed resistance to herbicides^[3].

p-Hydroxyphenylpyruvate dioxygenase (HPPD) is a known Fe (II)-containing non-heme oxygenase which has been recognized as a promising target for herbicide innovation^[4]. In most aerobic eukaryotic organisms, HPPD participates in the metabolic formation of tyrosine. In plants, at the catalysis of HPPD the natural substrate *p*-hydroxyphenylpyruvate acid can be converted to homogentisic acid which is transferred into plastids as plastoquinone and tocopherol. These two downstream products are the essential precursors for the pathway of photosynthesis in plants. Once HPPD is inhibited, it will adversely affect photosynthesis and thus lead to the death of plants associated with chlorosis. The herbicides targeting HPPD possess many advantages such as high herbicidal efficacy, broad weed control spectrum, low toxicity, and low risk of resistance development^[5,6]. More promisingly, HPPD-inhibiting herbicides have not shown cross-resistance with other classes of herbicides owing to their different modes of action, thereby exhibiting excellent control of some otherwise resistant weeds. Thus, HPPD-class herbicides may provide a solution for future

resistant weed management^[3,7]. The commercially available HPPD inhibitors can be divided into three types based on chemical structure: triketone-class herbicides (sulcotrione and mesotrione), pyrazole-class herbicides (pyrazolynate and topramazone) and isoxazole-class herbicides (isoxaflutole). Consequently, there is growing interest in studying HPPD and its inhibitors in many agrochemical companies and research institutions worldwide. The discovery of more novel active ingredients targeting HPPD will provide a foundation for the sustainable development of the herbicide industry.

It is well known that structural biology studies on action targets are of great importance in understanding the function of the protein and the interactions between the active molecules and the targets. Structure-based drug design (SBDD) is the purposeful design of drugs based on the three-dimensional structure of ligands and targets. Therefore, SBDD for improving the target affinity of the inhibitors is an effective tool to design novel drugs and agrochemicals with better performance^[8–11]. For example, the development of crizotinib (a clinical anticancer agent targeting *c*-MET kinase) was a successful application in drug discovery using SBDD^[12]. Based on preliminary research, we acquired and solved the crystal of *Arabidopsis thaliana* HPPD (*At*HPPD) complexed with the commercial HPPD inhibitor mesotrione (PDB ID: 5YWG, Fig. 1). Mesotrione is one of the highest selling herbicides globally with many advantages such as high efficacy, low toxicity, and high selectivity in maize. Unfortunately, it does not provide satisfactory control of some poaceous weeds^[13]. It is therefore important to design and develop more potent HPPD-inhibiting

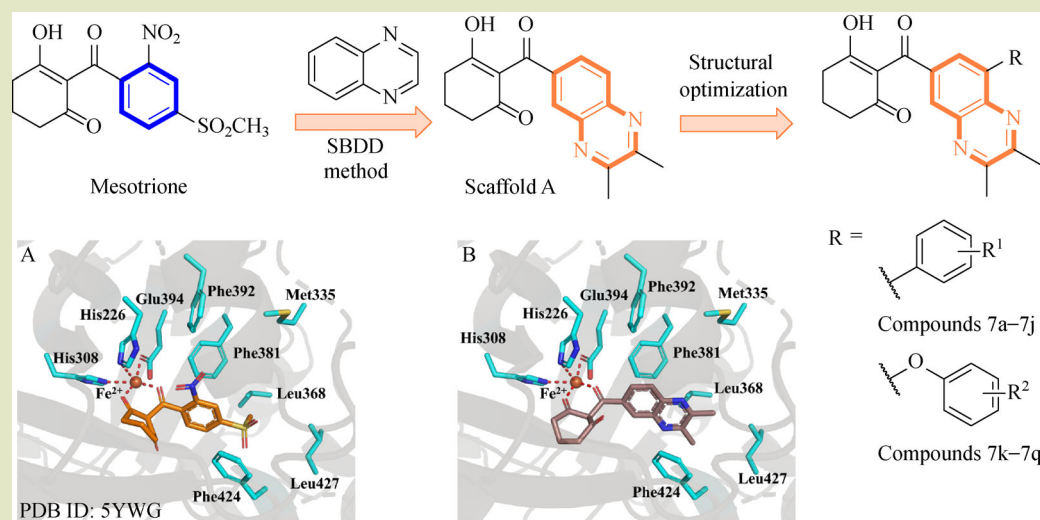


Fig. 1 Molecular design strategy of new triketone-quinoxaline HPPD inhibitors 7a–7q based on the commercial mesotrione using SBDD. (A) Binding model of *At*HPPD-mesotrione complex (PDB ID: 5YWG). (B) Docking model of the parent scaffold of the triketone-quinoxaline hybrids with *At*HPPD.

herbicides starting from mesotrione. It has been clearly demonstrated that the triketone moiety of mesotrione participates in bidentate chelation with the endogenous metal ion at the active site, and its benzene ring forms sandwich-like π - π stacking interaction with the residues Phe424 and Phe381. These interactions support the strong binding affinity of mesotrione with *At*HPPD. Starting from this structural information we attempted to employ an SBDD approach in the discovery of novel active molecules with HPPD inhibition, with the purpose of enhancing the target affinity of newly designed molecules based on mesotrione. The SBDD procedure we adopted aimed to retain the vital chelation of *At*HPPD with mesotrione while strengthening the π - π interaction through inserting a new π -conjugate heterocycle system into the triketone subunit.

Quinoxaline is a nitrogen-containing heterocyclic motif with a wide range of biological activities and has been used extensively in the fields of pesticides, medicines and materials^[14,15]. For example, S-2720 is a drug candidate with a quinoxaline scaffold that has been identified as a very potent HIV-1 reverse transcriptase inhibitor^[16]. Quizalofop-ethyl is an effective acetyl CoA carboxylase-inhibiting herbicide^[17]. The widely-acknowledged value of this benzoheterocycle triggered our research interest in extending its application in HPPD inhibitors. According to the design scheme given above, a quinoxaline ring was introduced into the active scaffold to replace the benzene ring of mesotrione, which possibly augments the π - π stacking interaction of the new molecule with Phe424 and Phe381. As a result, a triketone-quinoxaline hybrid (scaffold A, as shown in Fig. 1) was generated as a starting framework for new HPPD inhibitors. We also noticed that there is a large hydrophobic pocket in the direction of mesotrione extending toward the outside of the HPPD cavity, consisting of the hydrophobic residues Leu427, Phe424, Phe392, Phe381, Leu368 and Met335. Most importantly, this pocket is not occupied by mesotrione and the newly designed parent scaffold. This information will help in further increasing the binding affinity of triketone-quinoxalines with HPPD. In our plan the strong hydrophobic benzene ring, as an additional function group, was linked to the C-8 site of the quinoxaline ring of the newly designed core scaffold in the pose of biphenyl or diphenyl ether^[18]. Such modification aims to enhance the hydrophobic contact interaction of the new active molecules with the untouched hydrophobic residues (mentioned above). Hence, two types of novel HPPD inhibitors, namely (un)substituted phenyl-bearing triketone-quinoxaline derivatives (7a–7j) and (un)substituted phenoxy-bearing triketone-quinoxaline derivatives (7k–7q), were designed and synthesized. According to the outcome of enzyme inhibitory assays, these triketone-quinoxaline derivatives exhibited acceptable *At*HPPD inhibitory activity.

Some of these compounds were superior to mesotrione in *in vitro* inhibitory activity. These findings indicate that the triketone-quinoxaline hybrids, as a class of promising lead scaffold, possessed are potentially useful in herbicide discovery.

2 MATERIALS AND METHODS

2.1 Reagents and instruments

Analytically pure solvents were used for reactions, isolations and detections without further purification in the organic synthesis experiments. The purity of commercially available reagents was up to 95%. The extent of the reactions was checked by thin-layer chromatography (TLC). Usually, the spectra of ¹H/¹³C NMR for each tested compound were obtained with a Varian Mercury-Plus 400 or 600 (Varian Inc., Palo Alto, USA). The corresponding high-resolution mass spectra (HRMS) were determined with an Agilent 6224 LC-HRMS (Agilent, Santa Clara, USA) in ESI mode. Their melting points were measured and recorded using a Büchi-545 (Büchi, Flawil, Switzerland).

2.2 Synthetic chemistry

As shown in Fig. 2, the triketone-quinoxaline derivatives 7a–7q were synthesized via seven step reactions. 4-amino-3-nitrobenzoic acid (compound 1) was used as the starting material and a bromination reaction was conducted with *N*-bromosuccinimide (NBS) in *N,N*-dimethylformamide (DMF) under –5 °C, followed by the reduction of the nitro group to generate methyl 3,4-diamino-5-bromobenzoate (compound 3). The mixture of compound 3 and NH₄Cl was refluxed in methanol to obtain methyl 8-bromo-2,3-dimethylquinoxaline-6-carboxylate (compound 4)^[19]. Compounds 5a–5j were produced based on a known Suzuki-coupling reaction. In detail, compound 4 was reacted with (un)substituted phenyl boric acid in the presence of Pd(OAc)₂ and K₃PO₄·3H₂O to obtain the corresponding key quinoxaline intermediates containing phenyl group 5a–5j with acceptable yield^[20]. Another set of diphenyl ether-based quinoxaline compounds 5k–5q were constructed under microwave irradiation in the presence of 2-(dimethylamino)acetic acid hydrochloride (DMG·HCl) and CuI^[21,22]. Later, 2-chloro-1-methylpyridin-1-ium iodide (CMPI) was used as a condensing agent and the reaction of compounds 5a–5q with cyclohexane-1,3-dione resulted in enol esters 6a–6q with satisfactory yield. Finally, target compounds 7a–7q were obtained by a Fries rearrangement at the catalysis of acetone cyanohydrin. The chemical structures of all the acquired triketone-quinoxaline derivatives were characterized by means of ¹H/¹³C NMR and HRMS.

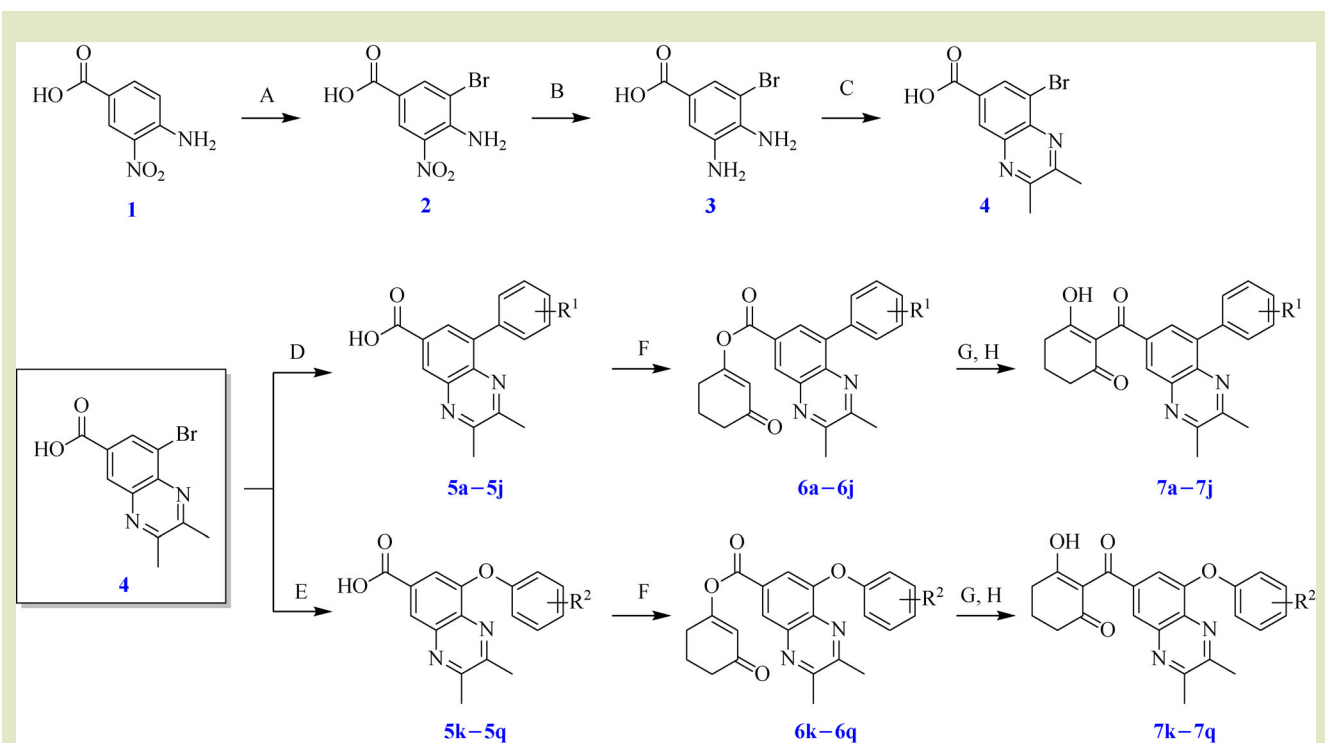


Fig. 2 The synthetic route of triketone-quinoxaline derivatives 7a–7q. Reagents and conditions: (A) NBS, DMF, -5°C ; (B) Raney Ni/ H_2 , MeOH, room temperature; (C) NH_4Cl , MeOH, reflux; (D) $\text{K}_3\text{PO}_4 \cdot 3\text{H}_2\text{O}$, $\text{Pd}(\text{OAc})_2$, reflux; (E) $\text{DMG} \cdot \text{HCl}$, CuI , Cs_2CO_3 , dioxane, $126\text{--}130^{\circ}\text{C}$, microwave; (F) CMPI , cyclohexane-1,3-dione, Et_3N , dichloromethane, room temperature; (G) Et_3N , acetone cyanohydrin, CH_3CN , $25\text{--}30^{\circ}\text{C}$; (H) $1\text{ mol} \cdot \text{L}^{-1}$ HCl .

2.3 Molecular docking

The cocrystal structure of *At*HPPD-mesotrione (5YWG) was downloaded from the RCSB Protein Data Bank. The three-dimensional models of the compounds were visualized by two commonly used computational software packages, SYBYL 7.3 (Tripos, Inc., St. Louis, MO) and GOLD 3.0 (GlaxoSmithKline plc, Brentford, UK). The Fe(II), the catalytic center at the active site, was used to define the binding site and the radius of the active site was installed to 10 \AA . A total of 100 runs were calculated based on a genetic algorithm. Finally, the highest ranked rational conformation of the chosen compounds was selected as the final binding confirmation by comparing the crystal complex of *At*HPPD-mesotrione^[23,24].

2.4 Binding free energy calculation

The binding free energy $\Delta G_{\text{binding}}$ was calculated by the molecular mechanics Poisson-Boltzmann surface area (MM-PBSA) method in Amber16 (Amber, San Francisco, CA) as follows:

$$\begin{aligned} \Delta G_{\text{binding}} &= \Delta H - T\Delta S = \Delta E_{\text{MM}} + \Delta G_{\text{sol}} - T\Delta S \\ &= \Delta G_{\text{polar}} + \Delta G_{\text{nonpolar}} - T\Delta S \end{aligned} \quad (1)$$

$$\Delta E_{\text{MM}} = \Delta E_{\text{ele}} + \Delta E_{\text{vdw}} \quad (2)$$

$$\Delta G_{\text{sol}} = \Delta G_{\text{PB}} + \Delta G_{\text{SA}} \quad (3)$$

$$\Delta G_{\text{polar}} = \Delta G_{\text{ele}} + \Delta G_{\text{PB}} \quad (4)$$

$$\Delta G_{\text{nonpolar}} = \Delta G_{\text{vdw}} + \Delta G_{\text{SA}} \quad (5)$$

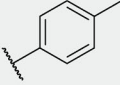
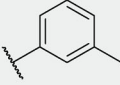
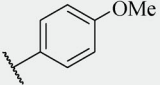
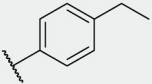
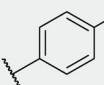
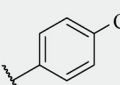
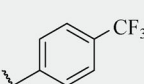
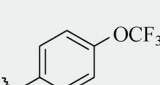
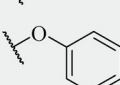
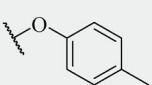
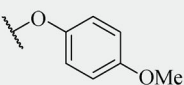
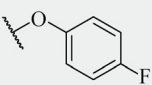
where $\Delta G_{\text{binding}}$, ΔH and ΔS are the binding free energy, enthalpy, and entropy of the ligand, respectively. The molecular mechanics (MM) energy in the gas phase ΔE_{MM} is the sum of electrostatic energy ΔE_{ele} and van der Waals energy ΔE_{vdw} . Solvation free energy ΔG_{sol} is the sum of the polar solvation energy ΔG_{PB} and the nonpolar contribution ΔG_{SA} between the solute and the continuum solvent. The polar contribution ΔG_{polar} is the sum of ΔE_{ele} and ΔG_{PB} . The nonpolar energy $\Delta G_{\text{nonpolar}}$ is the sum of ΔG_{vdw} and ΔG_{SA} .

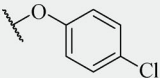
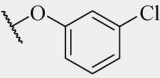
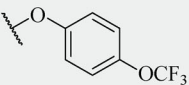
2.5 *At*HPPD inhibitory assay

*At*HPPD was used as the target protein to assess the in vitro inhibitory activity of target compounds 7a–7q. The commercially available herbicide mesotrione was included as a positive control. The expression and purification of *At*HPPD were conducted according to previous publications^[8,23–26]. On the

basis of the purified *At*HPPD the bioactivity investigations of the synthesized compounds were conducted using a coupled enzyme experiment^[13,27]. The half-maximum inhibitory concentration (IC_{50}) was used to measure the enzyme inhibitory activity of all the synthesized compounds and the control and the corresponding values are listed in Table 1.

Table 1 Inhibitory activity of triketone-quinoxaline derivatives against *At*HPPD

Compound	R	Yield (%)	CLogP	IC_{50} for <i>At</i> HPPD inhibition ($\mu\text{mol}\cdot\text{L}^{-1}$)
7a		40	4.04	0.891 ± 0.021
7b		46	4.54	0.423 ± 0.036
7c		45	4.54	0.643 ± 0.036
7d		52	4.24	0.317 ± 0.010
7e		54	3.97	0.492 ± 0.024
7f		57	5.07	0.555 ± 0.026
7g		45	4.19	0.533 ± 0.021
7h		48	4.76	0.595 ± 0.025
7i		40	4.93	0.353 ± 0.033
7j		44	5.08	0.823 ± 0.066
7k		42	4.25	0.791 ± 0.021
7l		49	4.75	0.533 ± 0.021
7m		40	4.17	0.565 ± 0.025
7n		39	4.40	0.406 ± 0.024

(Continued)				
Compound	R	Yield (%)	CLogP	IC ₅₀ for AtHPPD inhibition (μmol·L ⁻¹)
7o		43	4.97	0.643±0.036
7p		48	4.97	0.592±0.024
7q		50	5.28	0.460±0.029
Mesotrione	—	—	—	0.412±0.018

3 RESULTS AND DISCUSSION

3.1 Synthesis and determination

Synthesis of 4-amino-3-bromo-5-nitrobenzoic acid (compound 2): The mixture of NBS (107 g, 601 mmol) and DMF (250 mL) was added dropwise to a solution of 4-amino-3-nitrobenzoic acid (100 g, 549 mmol) in DMF (250 mL) and stirred vigorously at -5 °C for 12 h. The reaction process was monitored by TLC and the mixture was then poured into ice water (2 L) after completion, resulting in a yellow solid. The solid was filtered to give the desired compound 2 with a yield of 98%. ¹H NMR (400 MHz, DMSO-*d*₆): δ 8.30 (s, 1H) 7.76 (s, 1H).

Synthesis of 3,4-diamino-5-bromobenzoic acid (compound 3): Raney Ni (5 wt%) was added to a suspension of compound 2 (50 g, 192 mmol) in methanol (200 mL) and stirred at room temperature for 20 h in a hydrogen atmosphere. After the reaction was confirmed by TLC detection the mixture was filtered to give a yellow filtrate which was evaporated under vacuum and further purified using silica gel column chromatography with hexane:acetone (20:1) to give the desired reduction compound 3 (42.1 g, yield 95%) as a yellow solid. ¹H NMR (400 MHz, DMSO-*d*₆): δ 6.92 (s, 1H) 6.80 (s, 1H).

Synthesis of 8-bromo-2,3-dimethylquinoxaline-6-carboxylic acid (compound 4): Biacetyl (19.4 g, 225 mmol) and NH₄Cl (3.37 g, 63 mmol) were added to a suspension of compound 3 (40 g, 173 mmol) in 200 mL of MeOH. The mixture was vigorously stirred under reflux. During the reaction a large amount of solid was generated. Half of the solvent was removed under vacuum and the remaining residue was filtered to produce compound 4 as a light powder with a yield of 73%. ¹H NMR

(400 MHz, DMSO-*d*₆): δ 8.88 (s, 1H) 8.72 (s, 1H) 2.76 (s, 3H) 2.75 (s, 3H).

General synthesis procedure for compounds 5a–5j: (Un) substituted phenylboronic acid (4.5 mmol), K₃PO₄·3H₂O (6 mmol), and Pd(OAc)₂ (0.01 mmol) were added to a mixture of intermediate 4 (3 mmol), DMF (20 mL) and H₂O (10 mL) and the reaction system was heated to reflux. When the reaction was complete the suspension was filtered and the filtrate was extracted with ethyl acetate twice (2 × 10 mL). Finally, the compounds 5a–5j were obtained by acidifying the resultant water phase using 2 mol·L⁻¹ HCl (yield 72%–85%).

General procedure for the synthesis of coupling compounds 5k–5q: CuI (0.25 mmol), DMG·HCl (0.25 mmol), and Cs₂CO₃ (2.5 mmol) were added to a suspension of compound 4 (2 mmol) in 3 mL of dry 1,4-dioxane in a microwave tube under a nitrogen atmosphere. The mixture was stirred vigorously at 126 °C for 15 min and further stirred at 130 °C for 10 min. After the completion of this reaction, water (10 mL) was added to the tube and the mixture filtered. The filtrate was extracted with ethyl acetate twice (2 × 10 mL) and the resultant water phase was acidified with 2 mol·L⁻¹ HCl which generated the solid and finally gave the corresponding products 5k–5q through filtration (yield 65%–78%).

General synthesis procedure for compounds 6a–6q: CMPI (2 mmol) and triethylamine (2 mmol) were added to a solution of compounds 5a–5q (1 mmol) in 25 mL of dry dichloromethane. The mixture was stirred vigorously at room temperature. After 8 h, cyclohexane-1,3-dione (1.2 mmol) and triethylamine (2 mmol) were added in turn. After the reaction was completed by TLC detection, 20 mL of saturated NaHCO₃

aqueous solution was added to the suspension. The water phase was extracted with dichloromethane twice (2×20 mL) and the combined organic phase was washed with saturated NaCl aqueous solution. Undergoing desiccation and concentration of the organic phase, the desired products 6a–6q were further purified using silica gel column chromatography with a yield of 51%–78%.

3-Oxocyclohex-1-en-1-yl 2,3-dimethyl-8-phenylquinoxaline-6-carboxylate (compound 6a): Yield 51%; Yellow solid. ^1H NMR (400 MHz, CDCl_3) δ 8.76 (s, 1H), 8.33 (s, 1H), 7.77–7.70 (m, 2H), 7.57–7.46 (m, 2H), 7.51–7.42 (m, 1H), 6.14 (s, 1H), 2.78 (s, 3H), 2.77–2.70 (m, 5H), 2.50 (t, $J = 6.4$ Hz, 2H), 2.17 (quint, $J = 6.4$ Hz, 2H).

3-Oxocyclohex-1-en-1-yl 2,3-dimethyl-8-(p-tolyl)quinoxaline-6-carboxylate (compound 6b): Yield 74%; White solid. ^1H NMR (600 MHz, CDCl_3) δ 8.75 (s, 1H), 8.31 (s, 1H), 7.64 (d, $J = 7.8$ Hz, 2H), 7.33 (d, $J = 7.8$ Hz, 2H), 6.14 (s, 1H), 2.78 (s, 3H), 2.77–2.71 (m, 5H), 2.49 (t, $J = 6.6$ Hz, 2H), 2.46 (s, 3H), 2.17 (quint, $J = 6.6$ Hz, 2H).

3-Oxocyclohex-1-en-1-yl 2,3-dimethyl-8-(m-tolyl)quinoxaline-6-carboxylate (compound 6c): Yield 78%; White solid. ^1H NMR (600 MHz, CDCl_3) δ 8.14 (s, 1H), 7.81 (s, 1H), 7.53 (d, $J = 1.2$ Hz, 1H), 7.52 (s, 1H), 7.45–7.32 (m, 1H), 7.24 (d, $J = 7.8$ Hz, 1H), 6.13 (s, 1H), 2.79 (t, $J = 6.0$ Hz, 2H), 2.75 (s, 3H), 2.70 (s, 3H), 2.53 (t, $J = 6.6$ Hz, 2H), 2.44 (s, 3H), 2.11 (quint, $J = 6.6$ Hz, 2H).

3-Oxocyclohex-1-en-1-yl 2,3-dimethyl-8-(o-tolyl)quinoxaline-6-carboxylate (compound 6d): Yield 55%; White solid. ^1H NMR (600 MHz, CDCl_3) δ 8.78 (s, 1H), 8.17 (s, 1H), 7.40–7.36 (m, 1H), 7.34 (d, $J = 8.4$ Hz, 1H), 7.31 (d, $J = 7.2$ Hz, 1H), 7.29–7.27 (m, 1H), 6.13 (s, 1H), 2.77 (s, 3H), 2.73 (t, $J = 6.0$ Hz, 2H), 2.66 (s, 3H), 2.49 (t, $J = 6.0$ Hz, 2H), 2.16 (quint, $J = 6.6$ Hz, 2H), 2.05 (s, 3H).

3-Oxocyclohex-1-en-1-yl 8-(4-methoxyphenyl)-2,3-dimethylquinoxaline-6-carboxylate (compound 6e): Yield 59%; White solid. ^1H NMR (600 MHz, CDCl_3) δ 8.11 (s, 1H), 7.79 (s, 1H), 7.69 (d, $J = 8.4$ Hz, 2H), 7.03 (d, $J = 8.4$ Hz, 2H), 6.14 (s, 1H), 3.88 (s, 3H), 2.79 (t, $J = 5.4$ Hz, 2H), 2.75 (s, 3H), 2.53 (s, 3H), 2.79 (t, $J = 6.0$ Hz, 2H), 2.11 (quint, $J = 6.0$ Hz, 2H).

3-Oxocyclohex-1-en-1-yl 8-(4-ethylphenyl)-2,3-dimethylquinoxaline-6-carboxylate (compound 6f): Yield 64%; White solid. ^1H NMR (600 MHz, CDCl_3) δ 8.76 (s, 1H), 8.35 (s, 1H), 7.71 (d, $J = 7.8$ Hz, 2H), 7.39 (d, $J = 7.8$ Hz, 2H), 6.17 (s, 1H), 2.83–2.79 (m, 5H), 2.79–2.75 (m, 5H), 2.52 (t, $J = 6.6$ Hz, 2H), 2.19 (quint,

$J = 6.6$ Hz, 2H), 1.36 (t, $J = 7.8$ Hz, 3H).

3-Oxocyclohex-1-en-1-yl 8-(4-fluorophenyl)-2,3-dimethylquinoxaline-6-carboxylate (compound 6g): Yield 58%; White solid. ^1H NMR (600 MHz, CDCl_3) δ 8.75 (s, 1H), 8.29 (s, 1H), 7.72 (dd, $J = 8.4, 6.0$ Hz, 2H), 7.21 (dd, $J = 8.4, 6.0$ Hz, 2H), 6.14 (s, 1H), 2.78 (s, 3H), 2.77–2.66 (m, 5H), 2.50 (t, $J = 6.6$ Hz, 2H), 2.17 (quint, $J = 6.6$ Hz, 2H).

3-Oxocyclohex-1-en-1-yl 8-(4-chlorophenyl)-2,3-dimethylquinoxaline-6-carboxylate (compound 6h): Yield 53%; White solid. ^1H NMR (600 MHz, CDCl_3) δ 8.76 (s, 1H), 8.29 (s, 1H), 7.72 (d, $J = 8.4$ Hz, 2H), 7.21 (d, $J = 8.4$ Hz, 2H), 6.14 (s, 1H), 2.78 (s, 3H), 2.77–2.68 (m, 5H), 2.50 (t, $J = 6.6$ Hz, 2H), 2.17 (quint, $J = 6.6$ Hz, 2H).

3-Oxocyclohex-1-en-1-yl 2,3-dimethyl-8-(4-(trifluoromethyl)phenyl)quinoxaline-6-carboxylate (compound 6i): Yield 54%; White solid. ^1H NMR (600 MHz, CDCl_3) δ 8.19 (s, 1H), 7.84 (s, 2H), 7.81 (d, $J = 0.6$ Hz, 1H), 7.74 (d, $J = 7.8$ Hz, 2H), 6.14 (s, 1H), 2.81 (t, $J = 12.0$ Hz, 2H), 2.76 (s, 3H), 2.71 (s, 3H), 2.54 (t, $J = 6.6$ Hz, 2H), 2.12 (quint, $J = 7.2$ Hz, 2H).

3-Oxocyclohex-1-en-1-yl 2,3-dimethyl-8-(4-(trifluoromethoxy)phenyl)quinoxaline-6-carboxylate (compound 6j): Yield 61%; White solid. ^1H NMR (600 MHz, CDCl_3) δ 8.77 (s, 1H), 8.30 (s, 1H), 7.77 (d, $J = 8.4$ Hz, 2H), 7.36 (d, $J = 8.4$ Hz, 2H), 6.14 (s, 1H), 2.79 (s, 3H), 2.77–2.70 (m, 5H), 2.50 (t, $J = 7.2$ Hz, 2H), 2.17 (quint, $J = 6.6$ Hz, 2H).

3-Oxocyclohex-1-en-1-yl 2,3-dimethyl-8-phenoxyquinoxaline-6-carboxylate (compound 6k): Yield 55%; White solid. ^1H NMR (600 MHz, CDCl_3) δ 8.50 (s, 1H), 7.54 (s, 1H), 7.46–7.39 (m, 2H), 7.24 (t, $J = 7.2$ Hz, 1H), 7.17 (d, $J = 7.8$ Hz, 2H), 6.05 (s, 1H), 2.83 (s, 3H), 2.81 (s, 3H), 2.66 (t, $J = 6.0$ Hz, 2H), 2.46 (t, $J = 6.6$ Hz, 2H), 2.12 (quint, $J = 6.6$ Hz, 2H).

3-Oxocyclohex-1-en-1-yl 2,3-dimethyl-8-(p-tolyloxy)quinoxaline-6-carboxylate (compound 6l): Yield 66%; White solid. ^1H NMR (600 MHz, CDCl_3) δ 8.42 (s, 1H), 7.46 (s, 1H), 7.24 (d, $J = 8.0$ Hz, 2H), 7.06 (d, $J = 8.0$ Hz, 2H), 6.06 (s, 1H), 3.83 (s, 3H), 2.82 (s, 3H), 2.76 (s, 3H), 2.73 (t, $J = 6.0$ Hz, 2H), 2.45 (t, $J = 8.4$ Hz, 2H), 2.04 (quint, $J = 6.6$ Hz, 2H).

3-Oxocyclohex-1-en-1-yl 8-(4-methoxyphenoxy)-2,3-dimethylquinoxaline-6-carboxylate (compound 6m): Yield 62%; White solid. ^1H NMR (600 MHz, CDCl_3) δ 8.42 (s, 1H), 7.40 (s, 1H), 7.19 (d, $J = 7.8$ Hz, 2H), 6.96 (d, $J = 7.8$ Hz, 2H), 6.05 (s, 1H), 2.80 (s, 3H), 2.75 (s, 3H), 2.72 (t, $J = 6.0$ Hz, 2H), 2.45 (t, $J = 6.6$ Hz, 2H), 2.36 (s, 3H), 2.04 (quint, $J = 6.0$ Hz, 2H).

3-Oxocyclohex-1-en-1-yl 8-(4-fluorophenoxy)-2,3-dimethylquinoxaline-6-carboxylate (compound 6n): Yield 70%; White solid. ^1H NMR (600 MHz, CDCl_3) δ 8.53 (s, 1H), 7.56 (s, 1H), 7.38 (dd, $J = 8.4, 6.0$ Hz, 2H), 7.09 (dd, $J = 8.4, 6.0$ Hz, 2H), 6.06 (s, 1H), 2.83 (s, 3H), 2.81 (s, 3H), 2.68 (t, $J = 6.6$ Hz, 2H), 2.47 (t, $J = 6.6$ Hz, 2H), 2.13 (quint, $J = 6.6$ Hz, 2H).

3-Oxocyclohex-1-en-1-yl 8-(3-chlorophenoxy)-2,3-dimethylquinoxaline-6-carboxylate (compound 6o): Yield 62%; White solid. ^1H NMR (400 MHz, CDCl_3) δ 8.54 (s, 1H), 7.61 (s, 1H), 7.24 (d, $J = 7.6$ Hz, 1H), 7.16–7.12 (m, 2H), 6.06 (s, 1H), 2.83 (s, 3H), 2.79 (s, 3H), 2.69 (t, $J = 6.4$ Hz, 2H), 2.45 (t, $J = 6.4$ Hz, 2H), 2.05 (quint, $J = 6.6$ Hz, 2H).

3-Oxocyclohex-1-en-1-yl 8-(4-chlorophenoxy)-2,3-dimethylquinoxaline-6-carboxylate (compound 6p): Yield 56%; White solid. ^1H NMR (600 MHz, CDCl_3) δ 8.50 (s, 1H), 8.02 (s, 1H), 7.47 (d, $J = 7.8$ Hz, 2H), 7.14 (d, $J = 7.8$ Hz, 2H), 6.06 (s, 1H), 2.78 (s, 3H), 2.76 (s, 3H), 2.73 (t, $J = 6.0$ Hz, 2H), 2.45 (t, $J = 6.0$ Hz, 2H), 2.04 (quint, $J = 6.6$ Hz, 2H).

3-Oxocyclohex-1-en-1-yl 2,3-dimethyl-8-(4-(trifluoromethoxy)phenoxy)quinoxaline-6-carboxylate (compound 6q): Yield 54%; White solid. ^1H NMR (400 MHz, CDCl_3) δ 8.54 (s, 1H), 7.62 (s, 1H), 7.25 (d, $J = 7.2$ Hz, 2H), 7.15 (d, $J = 7.6$ Hz, 2H), 6.07 (s, 1H), 2.80 (s, 3H), 2.75 (s, 3H), 2.68 (t, $J = 6.0$ Hz, 2H), 2.47 (t, $J = 6.4$ Hz, 2H), 2.13 (quint, $J = 6.4$ Hz, 2H).

General procedure for the synthesis of compounds 7a–7q: Triethylamine (2 mmol) and acetone cyanohydrin (0.1 mmol) were added to a mixture of compounds 6a–6q (0.5 mmol) in 15 mL of dry CH_3CN and stirred vigorously at room temperature for 5–14 h. The solvent and triethylamine were evaporated under vacuum. The residue was dissolved in dichloromethane to which 1 mol·L⁻¹ HCl was subsequently added and then extracted with dichloromethane. The resulting organic phase was dried with anhydrous Na_2SO_4 and the solvent was evaporated in vacuo. Finally, the residue obtained was recrystallized with methanol and then purified using silica gel column chromatography with hexane:acetone (25:1) to produce the compounds 7a–7q with yields of 39%–57%.

2-(2,3-Dimethyl-8-phenylquinoxaline-6-carbonyl)-3-hydroxycyclohex-2-en-1-one (compound 7a): Yield 40%; Yellow solid; m.p. 190–191 °C. ^1H NMR (400 MHz, CDCl_3) δ 16.84 (s, 1H), 8.15 (s, 1H), 7.82 (s, 1H), 7.73 (d, $J = 7.6$ Hz, 2H), 7.56–7.49 (m, 2H), 7.46–7.36 (m, 1H), 2.79 (t, $J = 6.4$ Hz, 2H), 2.75 (s, 3H), 2.70 (s, 3H), 2.53 (t, $J = 6.4$ Hz, 2H), 2.11 (quint, $J = 6.4$ Hz, 2H). ^{13}C NMR (100 MHz, CDCl_3) δ 198.5, 196.5, 194.4, 155.1, 154.2, 140.8, 140.6, 139.8, 138.3, 138.2, 131.2, 128.8, 128.7, 128.2, 127.9,

113.8, 38.3, 32.6, 23.9, 23.3, 19.4. HRMS (ESI): Calcd. for $\text{C}_{23}\text{H}_{20}\text{N}_2\text{O}_3$ $[\text{M} + \text{H}]^+$ 373.1547. Found: 373.1553.

2-(2,3-Dimethyl-8-(o-tolyl)quinoxaline-6-carbonyl)-3-hydroxycyclohex-2-en-1-one (compound 7b): Yield 46%; Yellow solid; m.p. 172–174 °C. ^1H NMR (600 MHz, CDCl_3) δ 16.82 (s, 1H), 8.19 (s, 1H), 7.63 (s, 1H), 7.34 (d, $J = 7.2$ Hz, 1H), 7.33–7.27 (m, 3H), 2.77 (t, $J = 6.6$ Hz, 2H), 2.73 (s, 3H), 2.63 (s, 3H), 2.51 (t, $J = 6.6$ Hz, 2H), 2.11–2.05 (m, 5H). ^{13}C NMR (100 MHz, CDCl_3) δ 198.4, 196.4, 194.1, 155.0, 154.0, 141.3, 140.2, 138.8, 138.0, 137.5, 130.8, 129.8, 129.1, 128.7, 127.8, 125.4, 113.6, 38.1, 32.5, 23.7, 23.2, 20.9, 19.2. HRMS (ESI): Calcd. for $\text{C}_{24}\text{H}_{22}\text{N}_2\text{O}_3$ $[\text{M} + \text{H}]^+$ 387.1703. Found: 387.1701.

2-(2,3-Dimethyl-8-(m-tolyl)quinoxaline-6-carbonyl)-3-hydroxycyclohex-2-en-1-one (compound 7c): Yield 45%; Yellow solid; m.p. 168–179 °C. ^1H NMR (600 MHz, CDCl_3) δ 16.85 (s, 1H), 8.14 (s, 1H), 7.81 (s, 1H), 7.53 (d, $J = 1.2$ Hz, 1H), 7.52 (s, 1H), 7.48–7.36 (m, 1H), 7.24 (d, $J = 7.8$ Hz, 1H), 2.79 (t, $J = 6.0$ Hz, 2H), 2.75 (s, 3H), 2.70 (s, 3H), 2.53 (t, $J = 6.6$ Hz, 2H), 2.44 (s, 3H), 2.11 (quint, $J = 6.6$ Hz, 2H). ^{13}C NMR (100 MHz, CDCl_3) δ 198.2, 196.6, 194.2, 155.2, 154.3, 149.0, 140.6, 140.4, 138.2, 138.0, 136.8, 132.4, 129.1, 128.6, 120.5, 113.6, 38.2, 32.5, 23.8, 23.2, 21.5, 19.3. HRMS (ESI): Calcd. for $\text{C}_{24}\text{H}_{22}\text{N}_2\text{O}_3$ $[\text{M} + \text{Na}]^+$ 409.1523 Found: 409.1529.

2-(2,3-Dimethyl-8-(p-tolyl)quinoxaline-6-carbonyl)-3-hydroxycyclohex-2-en-1-one (compound 7d): Yield 52%; Yellow solid; m.p. 166–167 °C. ^1H NMR (600 MHz, CDCl_3) δ 16.81 (s, 1H), 8.13 (s, 1H), 7.80 (s, 1H), 7.63 (d, $J = 7.8$ Hz, 2H), 7.30 (d, $J = 7.8$ Hz, 2H), 2.79 (t, $J = 6.0$ Hz, 2H), 2.75 (s, 3H), 2.72 (s, 3H), 2.53 (t, $J = 6.0$ Hz, 2H), 2.44 (s, 3H), 2.10 (quint, $J = 6.0$ Hz, 2H). ^{13}C NMR (100 MHz, CDCl_3) δ 198.4, 196.4, 194.2, 154.8, 153.9, 140.8, 140.5, 139.6, 138.1, 137.6, 135.3, 130.9, 128.8, 128.42, 128.35, 113.6, 38.2, 32.5, 23.8, 23.2, 21.5, 19.3. HRMS (ESI): Calcd. for $\text{C}_{24}\text{H}_{22}\text{N}_2\text{O}_3$ $[\text{M} + \text{H}]^+$ 387.1703. Found: 387.1704.

3-Hydroxy-2-(8-(4-methoxyphenyl)-2,3-dimethylquinoxaline-6-carbonyl) cyclohex-2-en-1-one (compound 7e): Yield 54%; Yellow solid; m.p. 191–192 °C. ^1H NMR (600 MHz, CDCl_3) δ 16.82 (s, 1H), 8.11 (s, 1H), 7.79 (s, 1H), 7.69 (d, $J = 8.4$ Hz, 2H), 7.03 (d, $J = 8.4$ Hz, 2H), 3.88 (s, 3H), 2.79 (t, $J = 5.4$ Hz, 2H), 2.75 (s, 3H), 2.53 (s, 3H), 2.79 (t, $J = 6.0$ Hz, 2H), 2.11 (quint, $J = 6.0$ Hz, 2H). ^{13}C NMR (100 MHz, CDCl_3) δ 198.5, 196.4, 194.2, 159.4, 154.7, 153.9, 140.7, 140.5, 139.2, 138.1, 132.2, 130.6, 128.2, 128.1, 113.63, 113.59, 55.5, 38.2, 32.5, 23.8, 23.2, 19.3. HRMS (ESI): Calcd. for $\text{C}_{24}\text{H}_{22}\text{N}_2\text{O}_4$ $[\text{M} + \text{H}]^+$ 403.1652. Found: 403.1638.

2-(8-(4-Ethylphenyl)-2,3-dimethylquinoxaline-6-carbonyl)-3-

hydroxycyclohex-2-en-1-one (compound 7f): Yield 57%; Yellow solid; m.p. 159–160 °C. ¹H NMR (600 MHz, CDCl₃) δ 16.83 (s, 1H), 8.13 (s, 1H), 7.81 (s, 1H), 7.66 (d, *J* = 7.8 Hz, 2H), 7.32 (d, *J* = 7.8 Hz, 2H), 2.79 (t, *J* = 6.0 Hz, 2H), 2.75 (quint, *J* = 24.0 Hz, 2H), 2.74 (s, 3H), 2.70 (s, 3H), 2.53 (t, *J* = 6.6 Hz, 2H), 2.10 (quint, *J* = 6.6 Hz, 2H), 1.32 (t, *J* = 7.6 Hz, 3H). ¹³C NMR (100 MHz, CDCl₃) δ 198.4, 196.3, 194.1, 154.8, 153.9, 143.8, 140.7, 140.5, 139.5, 138.0, 135.5, 131.0, 128.4, 127.6, 113.6, 38.1, 32.4, 28.8, 23.7, 23.1, 19.2, 15.6. HRMS (ESI): Calcd. for C₂₅H₂₄N₂O₃ [M + Na]⁺ 423.1679. Found: 423.1680.

2-(8-(4-Fluorophenyl)-2,3-dimethylquinoxaline-6-carbonyl)-3-hydroxycyclohex-2-en-1-one (compound 7g): Yield 45%; Yellow solid; m.p. 174–175 °C. ¹H NMR (600 MHz, CDCl₃) δ 16.84 (s, 1H), 8.18 (s, 1H), 7.80 (s, 1H), 7.70 (dd, *J* = 8.4, 5.4 Hz, 2H), 7.17 (dd, *J* = 7.8, 6.0 Hz, 2H), 2.80 (t, *J* = 6.6 Hz, 2H), 2.75 (s, 3H), 2.71 (s, 3H), 2.54 (t, *J* = 6.6 Hz, 2H), 2.11 (quint, *J* = 6.4 Hz, 2H). ¹³C NMR (100 MHz, CDCl₃) δ 198.3, 196.5, 194.3, 164.0, 161.5, 155.0, 154.1, 140.54, 140.49, 138.5, 138.1, 134.11, 134.08, 132.7, 132.6, 128.8, 128.4, 115.1, 114.9, 113.6, 38.2, 32.5, 23.8, 23.2, 19.3. HRMS (ESI): Calcd. for C₂₃H₁₉FN₂O₃ [M + Na]⁺ 413.1272. Found: 413.1271.

2-(8-(4-Chlorophenyl)-2,3-dimethylquinoxaline-6-carbonyl)-3-hydroxycyclohex-2-en-1-one (compound 7h): Yield 48%; Yellow solid; m.p. 187–188 °C. ¹H NMR (600 MHz, CDCl₃) δ 16.83 (s, 1H), 8.15 (s, 1H), 7.78 (s, 1H), 7.67 (d, *J* = 8.4 Hz, 2H), 7.46 (d, *J* = 8.4 Hz, 2H), 2.80 (t, *J* = 6.0 Hz, 2H), 2.75 (s, 3H), 2.70 (s, 3H), 2.54 (t, *J* = 6.0 Hz, 2H), 2.11 (quint, *J* = 6.6 Hz, 2H). ¹³C NMR (100 MHz, CDCl₃) δ 198.3, 196.6, 194.3, 155.1, 154.2, 140.47, 140.45, 138.3, 138.2, 136.6, 133.9, 132.3, 129.0, 128.4, 128.3, 113.6, 38.2, 32.5, 23.8, 23.2, 19.3. HRMS (ESI): Calcd. for C₂₃H₁₉ClN₂O₃ [M + Na]⁺ 429.0976. Found: 429.0977.

2-(2,3-Dimethyl-8-(4-(trifluoromethyl)phenyl)quinoxaline-6-carbonyl)-3-hydroxycyclohex-2-en-1-one (compound 7i): Yield 40%; Yellow solid; m.p. 145–146 °C. ¹H NMR (600 MHz, CDCl₃) δ 16.80 (s, 1H), 8.19 (s, 1H), 7.84 (d, *J* = 7.8 Hz, 2H), 7.81 (s, 1H), 7.74 (d, *J* = 7.8 Hz, 2H), 2.81 (t, *J* = 6.0 Hz, 2H), 2.76 (s, 3H), 2.71 (s, 3H), 2.54 (t, *J* = 6.0 Hz, 2H), 2.12 (quint, *J* = 7.2 Hz, 2H). ¹³C NMR (100 MHz, CDCl₃) δ 198.5, 196.3, 194.2, 154.9, 153.9, 140.8, 140.4, 139.9, 138.10, 138.08, 137.6, 131.6, 128.6, 128.54, 128.48, 128.3, 127.9, 113.6, 38.2, 32.5, 23.8, 23.2, 21.8, 19.3. HRMS (ESI): Calcd. for C₂₄H₁₉F₃N₂O₃ [M + Na]⁺ 463.1240. Found: 463.1229.

2-(2,3-Dimethyl-8-(4-(trifluoromethoxy)phenyl)quinoxaline-6-carbonyl)-3-hydroxycyclohex-2-en-1-one (compound 7j): Yield 44%; Yellow solid; m.p. 159–160 °C. ¹H NMR (600 MHz, CDCl₃) δ 16.83 (s, 1H), 8.16 (s, 1H), 7.79 (s, 1H), 7.76 (d, *J*

= 9.0 Hz, 2H), 7.33 (d, *J* = 8.4 Hz, 2H), 2.80 (t, *J* = 6.6 Hz, 2H), 2.75 (s, 3H), 2.71 (s, 3H), 2.54 (t, *J* = 6.6 Hz, 2H), 2.11 (quint, *J* = 6.6 Hz, 2H). ¹³C NMR (100 MHz, CDCl₃) δ 198.2, 196.6, 194.3, 155.3, 154.4, 141.8, 140.5, 140.4, 138.2, 138.1, 131.4, 129.9, 129.6, 129.5, 128.7, 125.04, 125.01, 124.97, 124.9, 113.6, 38.2, 32.5, 23.8, 23.2, 19.3. HRMS (ESI): Calcd. for C₂₄H₁₉F₃N₂O₄ [M + H]⁺ 457.1370. Found: 457.1373.

2-(2,3-Dimethyl-8-phenoxyquinoxaline-6-carbonyl)-3-hydroxycyclohex-2-en-1-one (compound 7k): Yield 42%; Yellow solid; m.p. 172–173 °C. ¹H NMR (600 MHz, CDCl₃) δ 16.82 (s, 1H), 7.86 (s, 1H), 7.39 (d, *J* = 7.8 Hz, 2H), 7.23–7.16 (m, 3H), 7.05 (s, 1H), 2.80 (s, 3H), 2.76 (s, 3H), 2.73 (t, *J* = 6.0 Hz, 2H), 2.45 (t, *J* = 8.4 Hz, 2H), 2.04 (quint, *J* = 6.6 Hz, 2H). ¹³C NMR (100 MHz, DMSO-*d*₆) δ 194.5, 156.4, 155.9, 155.7, 152.7, 141.3, 137.1, 135.5, 130.3, 125.1, 124.3, 119.4, 115.8, 112.4, 32.8, 32.7, 23.2, 22.8, 20.2. HRMS (ESI): Calcd. for C₂₃H₂₀N₂O₄ [M + H]⁺ 389.1496. Found: 389.1488.

2-(2,3-Dimethyl-8-(*p*-tolylloxy)quinoxaline-6-carbonyl)-3-hydroxycyclohex-2-en-1-one (compound 7l): Yield 49%; Yellow solid; m.p. 148–149 °C. ¹H NMR (600 MHz, CDCl₃) δ 16.85 (s, 1H), 7.79 (s, 1H), 7.16 (d, *J* = 8.0 Hz, 2H), 6.94 (d, *J* = 8.0 Hz, 2H), 6.93 (s, 1H), 3.83 (s, 3H), 2.82 (s, 3H), 2.76 (s, 3H), 2.73 (t, *J* = 6.0 Hz, 2H), 2.45 (t, *J* = 8.4 Hz, 2H), 2.04 (quint, *J* = 6.6 Hz, 2H). ¹³C NMR (100 MHz, DMSO-*d*₆) δ 194.6, 156.3, 155.8, 155.5, 154.3, 148.8, 141.2, 136.8, 135.0, 124.4, 121.6, 115.4, 109.8, 55.5, 32.7, 32.6, 23.1, 22.8, 20.3. HRMS (ESI): Calcd. for C₂₄H₂₂N₂O₄ [M + Na]⁺ 425.1472. Found: 425.1453.

3-Hydroxy-2-(8-(4-methoxyphenoxy)-2,3-dimethylquinoxaline-6-carbonyl) cyclohex-2-en-1-one (compound 7m): Yield 40%; Yellow solid; m.p. 149–150 °C. ¹H NMR (600 MHz, CDCl₃) δ 16.83 (s, 1H), 7.81 (s, 1H), 7.19 (d, *J* = 8.0 Hz, 2H), 7.10 (d, *J* = 8.0 Hz, 2H), 7.01 (s, 1H), 2.80 (s, 3H), 2.75 (s, 3H), 2.72 (t, *J* = 6.0 Hz, 2H), 2.45 (t, *J* = 6.6 Hz, 2H), 2.36 (s, 3H), 2.04 (quint, *J* = 6.0 Hz, 2H). ¹³C NMR (100 MHz, DMSO-*d*₆) δ 195.0, 156.2, 156.0, 154.2, 153.9, 141.7, 137.3, 135.7, 134.1, 131.1, 125.2, 120.2, 116.3, 111.6, 55.4, 33.2, 23.6, 23.2, 20.8, 20.6. HRMS (ESI): Calcd. for C₂₄H₂₂N₂O₅ [M + Na]⁺ 425.1472. Found: 425.1464.

2-(8-(4-Fluorophenoxy)-2,3-dimethylquinoxaline-6-carbonyl)-3-hydroxycyclohex-2-en-1-one (compound 7n): Yield 39%; White solid; m.p. 169–170 °C. ¹H NMR (600 MHz, CDCl₃) δ 16.85 (s, 1H), 7.85 (s, 1H), 7.17 (dd, *J* = 8.4, 5.4 Hz, 2H), 7.08 (dd, *J* = 8.4, 5.4 Hz, 2H), 6.99 (s, 1H), 2.80 (s, 3H), 2.76 (s, 3H), 2.73 (t, *J* = 6.0 Hz, 2H), 2.45 (t, *J* = 8.4 Hz, 2H), 2.04 (quint, *J* = 6.6 Hz, 2H). ¹³C NMR (100 MHz, CDCl₃) δ 197.9, 195.9, 194.1, 160.8, 158.4, 155.2, 154.9, 153.2, 152.2, 141.4, 138.2, 135.2, 123.4, 122.2, 122.1, 116.7, 116.5, 113.6, 113.0, 38.0, 32.2, 23.7, 23.4, 19.2.

HRMS (ESI): Calcd. for $C_{23}H_{19}FN_2O_4$ $[M + Na]^+$ 429.1221. Found: 429.1214.

2-(8-(3-Chlorophenoxy)-2,3-dimethylquinoxaline-6-carbonyl)-3-hydroxycyclohex-2-en-1-one (compound 7o): Yield 43%; Yellow solid; m.p. 188–189 °C. 1H NMR (400 MHz, $CDCl_3$) δ 16.80 (s, 1H), 7.92 (s, 1H), 7.24–7.16 (m, 4H), 7.08 (s, 1H), 2.84–2.69 (m, 8H), 2.45 (t, $J = 6.4$ Hz, 2H), 2.05 (quint, $J = 6.4$ Hz, 2H). ^{13}C NMR (100 MHz, $CDCl_3$) δ 197.8, 196.0, 194.1, 155.3, 155.1, 152.1, 145.3, 141.5, 138.3, 135.5, 134.6, 124.0, 122.8, 121.2, 119.3, 114.6, 113.5, 38.0, 32.3, 23.8, 23.4, 19.2. HRMS (ESI): Calcd. for $C_{23}H_{19}ClN_2O_4$ $[M + Na]^+$ 445.0926. Found: 445.0934.

2-(8-(4-Chlorophenoxy)-2,3-dimethylquinoxaline-6-carbonyl)-3-hydroxycyclohex-2-en-1-one (compound 7p): Yield 48%; Yellow solid; m.p. 133–134 °C. 1H NMR (600 MHz, $CDCl_3$) δ 16.84 (s, 1H), 7.88 (s, 1H), 7.34 (d, $J = 7.8$ Hz, 2H), 7.12 (d, $J = 7.8$ Hz, 2H), 7.08 (s, 1H), 2.78 (s, 3H), 2.76 (s, 3H), 2.73 (t, $J = 6.0$ Hz, 2H), 2.45 (t, $J = 8.4$ Hz, 2H), 2.04 (quint, $J = 6.6$ Hz, 2H). ^{13}C NMR (100 MHz, $CDCl_3$) δ 197.8, 196.0, 194.1, 155.2, 155.0, 152.3, 141.4, 138.3, 135.4, 129.9, 123.8, 121.5, 117.3, 114.1, 113.5, 38.0, 32.2, 23.7, 23.4, 19.2. HRMS (ESI): Calcd. for $C_{23}H_{19}ClN_2O_4$ $[M + Na]^+$ 445.0926. Found: 445.0955.

2-(2,3-Dimethyl-8-(4-(trifluoromethoxy)phenoxy)quinoxaline-6-carbonyl)-3-hydroxycyclohex-2-en-1-one (compound 7q): Yield 50%; Yellow solid; m.p. 165–166 °C. 1H NMR (400 MHz, $CDCl_3$) δ 16.83 (s, 1H), 8.54 (d, $J = 0.8$ Hz, 1H), 7.62 (d, $J = 0.8$ Hz, 1H), 7.25 (d, $J = 7.2$ Hz, 2H), 7.15 (d, $J = 7.6$ Hz, 2H), 2.80 (s, 3H), 2.78 (s, 3H), 2.68 (t, $J = 6.0$ Hz, 2H), 2.47 (t, $J = 6.4$ Hz, 2H), 2.13 (quint, $J = 6.4$ Hz, 2H). ^{13}C NMR (100 MHz, $CDCl_3$) δ 197.7, 196.0, 194.0, 157.7, 155.2, 155.1, 151.6, 141.4, 138.3, 135.6, 135.1, 130.6, 124.2, 120.2, 118.0, 115.1, 113.5, 38.0, 32.2, 23.7, 23.3, 19.2. HRMS (ESI): Calcd. for $C_{23}H_{19}F_3N_2O_5$ $[M + Na]^+$ 495.1138. Found: 495.1134.

3.2 Enzyme inhibition and structure-activity relationship studies

From the inhibition data for compounds 7a–7q (Table 1), some of the synthesized compounds exhibited clear *At*HPPD inhibition, indicating that the newly designed molecules were HPPD inhibitors. Of these (un)substituted phenyl-containing triketone-quinoxalines, compounds 7d, 7i and 7n were more effective than mesotrione in inhibiting *At*HPPD activity. In particular, compound 7d ($IC_{50} = 0.317 \mu\text{mol}\cdot\text{L}^{-1}$) was the most inhibitory in this class and was slightly more inhibitory than mesotrione ($IC_{50} = 0.412 \mu\text{mol}\cdot\text{L}^{-1}$). In structure-activity relationships

studies we found that the position and the type of substituents of these compounds had important impacts on their activity. Specifically, the substituted phenyl derivatives were more inhibitory than the unsubstituted compound 7a. When a methyl group was introduced into the terminal phenyl group we observed that the *ortho*-methyl-substituted compound was considerably more inhibitory than compounds substituted at other positions, viz. *ortho*-methyl (7d, $IC_{50} = 0.317 \mu\text{mol}\cdot\text{L}^{-1}$) > *para*-methyl (7b, $IC_{50} = 0.423 \mu\text{mol}\cdot\text{L}^{-1}$) > *meta*-methyl (7c, $IC_{50} = 0.643 \mu\text{mol}\cdot\text{L}^{-1}$). When a halogen (F or Cl) was introduced into the phenyl group these compounds were almost equipotent enzyme inhibitors with the methyl-substituted derivatives (compounds 7b–7d). In addition, compound 7i with $-CF_3$ was strongly inhibitory to *At*HPPD with an IC_{50} of $0.353 \mu\text{mol}\cdot\text{L}^{-1}$. However, if the $-OCF_3$ was in the phenyl group the activity of the corresponding compound 7j ($IC_{50} = 0.823 \mu\text{mol}\cdot\text{L}^{-1}$) was declined somewhat.

Most of the diphenyl ether-containing triketone-quinoxaline series were strongly inhibitory to *At*HPPD. Specifically, the fluoro compound 7n ($IC_{50} = 0.406 \mu\text{mol}\cdot\text{L}^{-1}$) was more inhibitory than the chloro compounds 7o and 7p ($IC_{50} = 0.643$ and $0.592 \mu\text{mol}\cdot\text{L}^{-1}$, respectively). The fluoro compound 7n was more HPPD inhibitory than the derivatives with other types of substituents. An overall structure-activity relationship trend within the phenoxy-substituted triketone-quinoxaline derivatives can be summarized as follows: 4-F > 4- OCF_3 > 4- CH_3 > 4- OCH_3 > 3-Cl > 4-Cl > H.

3.3 Molecular simulation and docking studies

The most active compound 7d was docked into the active pocket of *At*HPPD to better understand the binding mode of the newly designed triketone-quinoxaline hybrids (Fig. 3A). It was clear that compound 7d was bound in the *At*HPPD active site and its two carbonyls of the triketone moiety formed strong chelation with Fe(II), combining with His226, His308 and Glu394. In addition, the quinoxaline part of compound 7d engaged two groups of π - π interaction with Phe424 and Phe381. Also, an additional phenyl on the quinoxaline skeleton embedded deeply into a hydrophobic cavity where compound 7d formed several hydrophobic contacts with the surrounding hydrophobic amino acid residues Met335, Leu368 and Leu427, as well as a set of favorable π - π interactions with Phe392. These interactions help to explain the molecular mechanism of compound 7d and its high level of inhibition of *At*HPPD.

We carried out the theoretical binding free energy calculation for compound 7d and mesotrione with HPPD using the MM-PBSA

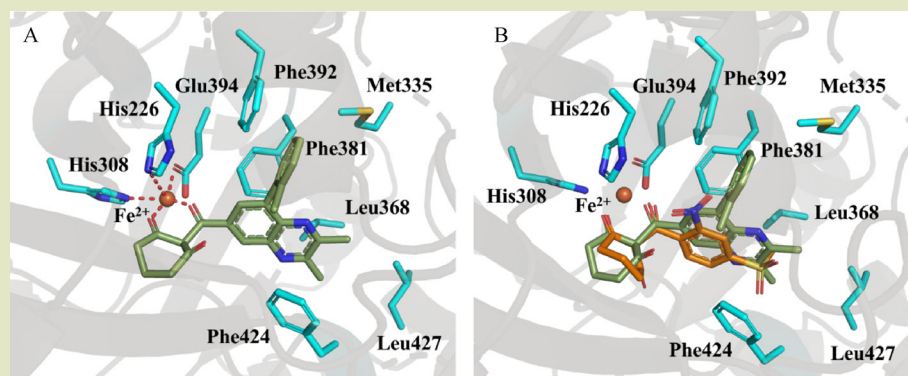


Fig. 3 (A) Binding mode of HPPD inhibitor 7d with AtHPPD. The chelation interactions are depicted as red dashed lines and compound 7d is shown as cyan. (B) Superposition of binding modes of compound 7d (cyan) and mesotrione (orange) in AtHPPD.

Table 2 Binding free energy calculations of compound 7d and mesotrione ($\text{kJ}\cdot\text{mol}^{-1}$)

Compound	$\Delta E_{\text{ele}}^{\text{a}}$	ΔE_{vdw}	ΔG_{PB}	ΔG_{SA}	ΔG_{polar}	$\Delta G_{\text{nonpolar}}$	ΔH	$-T\Delta S$	$\Delta G_{\text{binding}}$
7d	-194.7	-196.1	329.3	-28.3	134.6	-224.4	-89.8	45.6	-44.2
mesotrione	-187.3	-192.5	318.6	-18.5	131.3	-211.0	-79.7	46.0	-33.7

Note: ^aDetermined by the MM-PBSA method in Amber16.

method in order to illustrate the quantitative difference in binding. As shown in Table 2 the binding free energy of compound 7d ($-44.2 \text{ kJ}\cdot\text{mol}^{-1}$) was greater than that of mesotrione ($-33.7 \text{ kJ}\cdot\text{mol}^{-1}$), which was consistent with their experimental values. The $\Delta G_{\text{nonpolar}}$ of compound 7d ($-224.4 \text{ kJ}\cdot\text{mol}^{-1}$) was distinctly lower than polar contribution ΔG_{polar} ($134.6 \text{ kJ}\cdot\text{mol}^{-1}$), indicating the hydrophobic interaction of the ligand was critical in binding with AtHPPD. The hydrophobic interaction of mesotrione ($\Delta G_{\text{nonpolar}} = -211.0 \text{ kJ}\cdot\text{mol}^{-1}$) was weaker than that of compound 7d, leading directly to its poor binding ability. Overall, the result of binding free energy calculations reveals that compound 7d should be a more potent HPPD inhibitor than mesotrione.

According to the models of mesotrione and compound 7d bound to AtHPPD (Fig. 3B) we found that the quinoxaline of compound 7d had more compatible π -stacking between Phe424 and Phe381 in comparison to the benzene ring of mesotrione because of the larger contact surface of the quinoxaline scaffold. In addition, an apparent π - π interaction of the outstretched phenyl group on the quinoxaline of compound 7d with Phe392 was not observed in mesotrione, which also gave compound 7d an increased target binding potential. Overall, these findings

verify the reliability and feasibility of the HPPD inhibitor based SBDD and indicate that triketone-quinoxalines, represented by compound 7d, possess a suitable molecular basis for new herbicide discovery targeting HPPD.

4 CONCLUSIONS

A family of novel triketone HPPD inhibitors with quinoxaline as the core scaffold were predicted by SBDD and then synthesized in the process of new herbicide discovery. The HPPD inhibition assay shows that several triketone-quinoxaline derivatives had clear in vitro potency against AtHPPD. In particular, compound 7d ($\text{IC}_{50} = 0.317 \mu\text{mol}\cdot\text{L}^{-1}$) showed the strongest inhibition of HPPD and was superior to mesotrione, the commercial HPPD inhibitor. Molecular simulation was further conducted to determine the binding mode and molecular mechanism of compound 7d, providing useful information on the target binding to further assist in molecule design. These results and theoretical research indicate that the quinoxaline-containing triketone hybrids may serve as a class of valuable base structures for the discovery of new HPPD-inhibiting herbicides with improved performance.

Acknowledgements

This work was supported by the National Key R&D Program of China (2018YFD0200100), the National Natural Science Foundation of China (31901910, 21772058, and 21837001), and the China Postdoctoral Science Foundation (2018M642880).

Compliance with ethics guidelines

Baifeng Zheng, Yaochao Yan, Can Fu, Guangyi Huang, Long Zhao, Qiong Chen, Renyu Qu, and Guangfu Yang declare that they have no conflicts of interest or financial conflicts to disclose. This article does not contain any studies with human or animal subjects performed by any of the authors.

REFERENCES

1. Lamberth C, Jeanmart S, Luksch T, Plant A. Current challenges and trends in the discovery of agrochemicals. *Science*, 2013, **341**(6147): 742–746
2. Shaner D L. Lessons learned from the history of herbicide resistance. *Weed Science*, 2014, **62**(2): 427–431
3. Qu R Y, He B, Yang J F, Lin H Y, Yang W C, Wu Q Y, Li Q X, Yang G F. Where are the new herbicides? *Pest Management Science*, 2021, **77**(6): 2620–2625
4. Moran G R. 4-Hydroxyphenylpyruvate dioxygenase and hydroxymandelate synthase: exemplars of the α -keto acid dependent oxygenases. *Archives of Biochemistry and Biophysics*, 2014, **544**: 58–68
5. Ndikuryayo F, Kang W M, Wu F X, Yang W C, Yang G F. Hydrophobicity-oriented drug design (HODD) of new human 4-hydroxyphenylpyruvate dioxygenase inhibitors. *European Journal of Medicinal Chemistry*, 2019, **166**: 22–31
6. Ahrens H, Lange G, Müller T, Rosinger C, Willms L, van Almsick A. 4-Hydroxyphenylpyruvate dioxygenase inhibitors in combination with safeners: solutions for modern and sustainable agriculture. *Angewandte Chemie International Edition*, 2013, **52**(36): 9388–9398
7. van Almsick A. New HPPD-inhibitors—a proven mode of action as a new hope to solve current weed problems. *Outlooks on Pest Management*, 2009, **20**(1): 27–30
8. Qu R Y, Nan J X, Yan Y C, Chen Q, Ndikuryayo F, Wei X F, Yang W C, Lin H Y, Yang G F. Structure-guided discovery of silicon-containing subnanomolar inhibitor of hydroxyphenylpyruvate dioxygenase as a potential herbicide. *Journal of Agricultural and Food Chemistry*, 2021, **69**(1): 459–473
9. Qu R Y, Yang J F, Chen Q, Niu C W, Xi Z, Yang W C, Yang G F. Fragment-based discovery of flexible inhibitor targeting wild-type acetohydroxyacid synthase and P197L mutant. *Pest Management Science*, 2020, **76**(10): 3403–3412
10. Zhao P L, Wang L, Zhu X L, Huang X, Zhan C G, Wu J W, Yang G F. Subnanomolar inhibitor of cytochrome bc_1 complex designed by optimizing interaction with conformationally flexible residues. *Journal of the American Chemical Society*, 2010, **132**(1): 185–194
11. Hao G F, Wang F, Li H, Zhu X L, Yang W C, Huang L S, Wu J W, Berry E A, Yang G F. Computational discovery of picomolar $Q(\text{o})$ site inhibitors of cytochrome bc_1 complex. *Journal of the American Chemical Society*, 2012, **134**(27): 11168–11176
12. Cui J J, Tran-Dubé M, Shen H, Nambu M, Kung P P, Pairish M, Jia L, Meng J, Funk L, Botrous I, McTigue M, Grodsky N, Ryan K, Padrique E, Alton G, Timofeevski S, Yamazaki S, Li Q, Zou H, Christensen J, Mroczkowski B, Bender S, Kania R S, Edwards M P. Structure based drug design of crizotinib (PF-02341066), a potent and selective dual inhibitor of mesenchymal-epithelial transition factor (*c*-MET) kinase and anaplastic lymphoma kinase (ALK). *Journal of Medicinal Chemistry*, 2011, **54**(18): 6342–6363
13. Lin H Y, Yang J F, Wang D W, Hao G F, Dong J Q, Wang Y X, Yang W C, Wu J W, Zhan C G, Yang G F. Molecular insights into the mechanism of 4-hydroxyphenylpyruvate dioxygenase inhibition: enzyme kinetics, X-ray crystallography and computational simulations. *FEBS Journal*, 2019, **286**(5): 975–990
14. Pereira J A, Pessoa A M, Cordeiro M N D S, Fernandes R, Prudêncio C, Noronha J P, Vieira M. Quinoxaline, its derivatives and applications: a State of the Art review. *European Journal of Medicinal Chemistry*, 2015, **97**: 664–672
15. Carta A, Paglietti G, Rahbar Nikookar M E, Sanna P, Sechi L, Zanetti S. Novel substituted quinoxaline 1,4-dioxides with *in vitro* antimycobacterial and anticandida activity. *European Journal of Medicinal Chemistry*, 2002, **37**(5): 355–366
16. Montana M, Montero V, Khoumeri O, Vanelle P. Quinoxaline derivatives as antiviral agents: a systematic review. *Molecules*, 2020, **25**(12): 2784
17. Goud V V, Murade N B, Khakre M S, Patil A N. Efficacy of imazethapyr and quizalofop-ethyl herbicides on growth and yield of chickpea. *Bioscan*, 2013, **8**(3): 1015–1018
18. Chen T, Xiong H, Yang J F, Zhu X L, Qu R Y, Yang G F. Diaryl ether: a privileged scaffold for drug and agrochemical discovery. *Journal of Agricultural and Food Chemistry*, 2020, **68**(37): 9839–9877
19. Darabi H R, Tahoori F, Aghapoor K, Taala F, Mohsenzadeh F.

- $\text{NH}_4\text{Cl}-\text{CH}_3\text{OH}$: an efficient, acid- and metal-free catalyst system for the synthesis of quinoxalines. *Journal of the Brazilian Chemical Society*, 2008, **19**(8): 1646–1652
20. Li C, Li X Q, Zhang C. An aerobic ligandless palladium acetate catalysed Suzuki-Miyamura cross-coupling reaction in an aqueous solvent. *Journal of Chemical Research*, 2008, **2008**(9): 525–527
21. Ma D, Cai Q. N,N-dimethyl glycine-promoted Ullmann coupling reaction of phenols and aryl halides. *Organic Letters*, 2003, **5**(21): 3799–3802
22. Surati M A, Jauhari S, Desai K R. A brief review: microwave assisted organic reaction. *Archives of Applied Science Research*, 2012, **4**(1): 645–661
23. Wang D W, Lin H Y, Cao R J, Yang S G, Chen Q, Hao G F, Yang W C, Yang G F. Synthesis and herbicidal evaluation of triketone-containing quinazoline-2,4-diones. *Journal of Agricultural and Food Chemistry*, 2014, **62**(49): 11786–11796
24. Wang D W, Lin H Y, Cao R J, Chen T, Wu F X, Hao G F, Chen Q, Yang W C, Yang G F. Synthesis and herbicidal activity of triketone-quinoline hybrids as novel 4-hydroxyphenylpyruvate dioxygenase inhibitors. *Journal of Agricultural and Food Chemistry*, 2015, **63**(23): 5587–5596
25. Wang D W, Lin H Y, He B, Wu F X, Chen T, Chen Q, Yang W C, Yang G F. An efficient one-pot synthesis of 2-(aryloxyacetyl) cyclohexane-1,3-diones as herbicidal 4-hydroxyphenylpyruvate dioxygenase inhibitors. *Journal of Agricultural and Food Chemistry*, 2016, **64**(47): 8986–8993
26. Lin H Y, Chen X, Chen J N, Wang D W, Wu F X, Lin S Y, Zhan C G, Wu J W, Yang W C, Yang G F. Crystal structure of 4-hydroxyphenylpyruvate dioxygenase in complex with substrate reveals a new starting point for herbicide discovery. *Research*, 2019, **2019**: 2602414
27. Wu C S, Huang J L, Sun Y S, Yang D Y. Mode of action of 4-hydroxyphenylpyruvate dioxygenase inhibition by triketone-type inhibitors. *Journal of Medicinal Chemistry*, 2002, **45**(11): 2222–2228